Biophysical Journal Volume 103 November 2012 1880–1889

Phosphatidylserine Inhibits and Calcium Promotes Model Membrane Fusion

Pradip K. Tarafdar, Hirak Chakraborty, S. Moses Dennison, and Barry R. Lentz*
Department of Biochemistry and Biophysics and Program in Molecular and Cellular Biophysics, University of North Carolina at Chapel Hill, Chapel Hill, North Carolina

ABSTRACT PEG-mediated fusion of SUVs composed of dioleoylphosphatidylcholine, dioleoylphosphatidylethanolamine, sphingomyelin, cholesterol, and dioleoylphosphatidylserine was examined to investigate the effects of PS on the fusion mechanism. Lipid mixing, content mixing, and content leakage measurements were carried out with vesicles containing from 0 to 8 mol % PS and similar amounts of phosphatidylglycerol. Fitting these time courses globally to a 3-state (aggregate, intermediate, pore) sequential model established rate constants for each step and probabilities of lipid mixing, content mixing, and leakage in each state. Charged lipids inhibited both the rates of intermediate and pore formation as well as the extents of lipid and contents mixing, although electrostatics were not solely responsible for inhibition. Ca^{2+} counteracted this inhibition and increased the extent of fusion in the presence of PS to well beyond that seen in the absence of charged lipids. The effects of both PS and Ca^{2+} could be interpreted in terms of a previous proposal for the nature of lipid fluctuations that account for transition states for the two steps of the fusion process examined. The results suggest a more significant role for Ca^{2+}-lipid interactions than is acknowledged in current thinking about cell membrane fusion.

INTRODUCTION

Lipid bilayers form the core structure of the natural membranes that envelop eukaryotic cells and subdivide them into compartments with different structural and functional identities. The compositions of natural membranes are complex, with different lipids likely having distinct roles in membrane function. Phosphatidylcholine (PC), phosphatidylethanolamine (PE), SM, CH, PS are the predominant lipid species of mammalian membranes. Although PC, PE, and SM are zwitterionic, PS is anionic at physiological pH. Anionic (or acidic) lipids, when present in substantive amounts, should endow membranes with a sizable electrostatic potential, and facilitate avid binding of proteins with cationic clusters (2), although this view is not universal (3,4).

Membrane fusion is defined as the joining of two closely opposed lipid bilayers to form a single bilayer with minimal leakage of content. It is of central importance in the life of eukaryotic cells and also in the life cycle of such deadly viruses as influenza, human immunodeficiency virus, and hepatitis virus. Despite intensive research over the past 40 years, the detailed molecular mechanism of membrane fusion remains one of the central unsolved problems of membrane biophysics. Most current models of fusion assume that fusion proceeds through an initial stalk intermediate (5) that translates through a second intermediate (extended *trans*-membrane contact) (6) to fusion pores. The first and last steps (stalk and final pore formation, respectively) involve complex lipid rearrangements associated with changes in topology of the initial and final states for these steps (1). It is now reasonably well accepted that, although proteins catalyze the lipid rearrangements needed for all three steps (7), biomembrane fusion is exquisitely sensitive to lipid composition (8). PC and PE have opposing effects on bilayer hydration and therefore on the force required to bring bilayers to an interbilayer separation small enough for fusion to occur (9). Interestingly, the molar ratio of PC, PE, CH, and SM that proves optimal for PEG-mediated model membrane fusion (DOPC/DOPE/SM/CH: 35/30/15/20) is roughly that found in mammalian membranes (10), including neuronal membranes and synaptic vesicles. However, apart from the PC, PE, SM, and CH, synaptic vesicles contain a significant amount of PS (11), and incorporation of PS into vesicles composed of PC/PE/SM/CH (35:30:15:20) actually inhibited PEG-mediated model membrane fusion (10). Despite its inhibitory effect, PS is required for 1), Ca^{2+}-synaptotagmin-1 stimulated liposome fusion (12); 2), membrane binding of the fusion peptide of fertilin (13); and 3), synaptobrevin-modulated fusion of vesicles with plasma membrane (14); and 4), observing the ability of reconstituted neuronal SNARE proteins to promote PEG-mediated model membrane fusion (15). In part because of this, some of the earliest studies

Submitted June 21, 2012, and accepted for publication September 21, 2012.

*Correspondence: uncbrl@med.unc.edu

Hirak Chakraborty's present address is Centre for Cellular and Molecular Biology, Council of Scientific and Industrial Research, Hyderabad 500 007, India.

S. Moses Dennison's present address is Human Vaccine Institute, Duke University School of Medicine, Durham, North Carolina.

Abbreviations used: SUVs, small unilamellar vesicles; DOPC, 1,2-dioleoyl-3-*sn*-phosphatidylcholine; DOPE, 1,2-dioleoyl-3-*sn*-phosphatidylethanolamine; SM, sphingomyelin (bovine brain); CH, Cholesterol; DOPS, 1,2-dioleoyl-3-*sn*-phosphatidylserine; PS, phosphatidylserine; DOPG, 1,2-dioleoyl-3-*sn*-phosphatidylglycerol; PG, phosphatidylglycerol; TES, *N*- tris(hydroxymethyl)methyl}2-2-aminoethane sulfonic acid; PEG, poly(ethylene glycol); CM, contents mixing; LM, lipid mixing.

Editor: Lukas Tamm.

0006-3495/12/11/1880/10 $2.00
http://dx.doi.org/10.1016/j.bpj.2012.09.030

of fusion in model systems involved membranes composed of pure PS or of mixtures of 1/1 PS/PC treated with Ca^{2+} (16–18), although it was controversial whether the phenomenon studied was fusion or Ca^{2+}-induced phase separation (19,20). In addition, both the Ca^{2+} concentrations (1 mM for pure PS, >4 mM for PS/PC) and PS membrane contents used in these studies were far from those associated with fusion in vivo.

In view of this discussion, it is clearly of interest to understand how PS might modulate membrane fusion and how the presence of Ca^{2+} might influence the effects of PS. One possibility would be that the negative charge of PS should inhibit the close approach of membranes required to form the initial fusion intermediate (9), thus inhibiting the initial step (stalk formation) in fusion. Could PS also alter the subsequent step (pore formation) of the process? Because Ca^{2+} is known to form a stoichiometric complex with PS resulting in a semicrystalline dehydrated phase (19), could Ca^{2+} specifically modulate the effects of PS on fusion kinetics? Could the effects of Ca^{2+} on fusion of PS-containing model membranes provide insights into how Ca^{2+} might function in the fusion of mammalian membranes that contain ~8–10 mol % PS?

We recently showed that a one or two intermediate, sequential kinetic model that derives from the widely accepted stalk model for the fusion mechanism accounts for the time courses of PEG-induced fusion in a variety of systems (1,21,22). This model accounts for observed fusion kinetics in terms of an aggregated starting state (A), intermediate states (I_1 and I_2 for two intermediate or I for one intermediate model), and a final fusion pore state (FP). Using this approach, we have evaluated the effect of dioleoylphosphatidylserine (DOPS) and another acidic lipid (dioleoylphosphatidylglycerol, DOPG) on the kinetics of the fusion process in model membranes composed of dioleoylphosphatidylcholine (DOPC), dioleoylphosphatidylethanolamine (DOPE), SM, and CH. We have shown that 1), PS inhibits the rates and extents of both intermediate and FP formation, 2), inhibition of the first step involves a significant electrostatic effect but apparently effects that are specific to PS, 3), near physiological concentrations of free Ca^{2+} promote fusion if membranes are close, and 4), Ca^{2+} plus acidic lipid synergistically promote both the extent and rate of pore formation in a way that is specific for PS.

EXPERIMENTAL SECTION

Materials and Methods commonly used in our lab are described in the Supporting Material.

Measurement of vesicle aggregation and aggregate ensemble size

The time course of PEG-induced SUV aggregation (0.2 mM total lipid) was followed via turbidity at 400 nm (PerkinElmer Lambda 25 spectrophotometer; PerkinElmer), whereas SUV aggregate size was determined by quasielastic dynamic light scattering using a DynaPro Plate instrument (Wyatt Technology).

Measurement of free calcium concentration

Free calcium concentrations in buffer (10 mM TES, 100 mM NaCl, 1mM EDTA) with SUVs (0.2 mM lipid) were determined at different added calcium concentrations in the range of 10 μM to 10 mM using a standard curve (Fig. S3 in the Supporting Material) constructed with the use of a calcium selective electrode (detectION, Nico Scientific, Philadelphia, PA).

Recording and analyzing fusion time courses

Experimentally, the fusion process was tracked by monitoring LM between vesicle membranes LM, CM between vesicle compartments and content leakage (L)(1). We analyzed our kinetic data in terms of the sequential one intermediate model described in detail earlier (21). SUVs (0.2 mM lipid) are brought rapidly into close contact by mixing with PEG to form an aggregated (A) state. In our model, the A state forms a fusion intermediate (I, stalk-like) at a rate k_1, which then converts to a FP at rate k_3 (see following scheme). Note that the second rate is written as k_3 for consistency with the general treatment in which the FP-forming step follows a second intermediate and is labeled 3 (1,21).

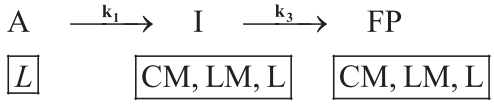

CM and LM are considered to occur in the states with probabilities α_i (CM) and β_i (LM), whereas leakage from each state is considered to occur with a rate λ_i. In all, a total of seven parameters (two rate constants, two α_i, β_i, and three λ_i) are required to describe three double exponential curves, which in theory can define 9–12 parameters, guaranteeing that the model is not underdetermined (1). We note that the events we observe (CM, LM, L) are not reversible, and thus our observations are not linear in intermediate and/or pore formation (i.e., once an intermediate or pore forms between two vesicles, formation of a second intermediate or pore between these same two vesicles is invisible). This nonlinearity of experimental observables with initial intermediate or FP formation is properly accounted for in Eqs. 6 and 7 and Appendix I of Weinreb et al. (21). The model and details of the analysis are described in more detail in the Supporting Material.

RESULTS

Effect of DOPS on PEG-mediated SUV fusion

Fusion of SUVs with an optimal fusogenic composition (DOPC/DOPE/SM/CH:35/30/15/20) was inhibited by

inclusion of PS (DOPC/DOPE/SM/CH/PS:30/25/15/20/10) in single-point assays at different concentrations of PEG, a situation that we speculated (10) might be due to charged lipid interfering with interbilayer close contact required for fusion (9). In initial experiments at 0.2 mM lipid, 23°C, and 5 wt % PEG, at which we carry out most kinetic studies, the rate of fusion of PS-containing vesicles were too slow for useful measurements. For this reason, fusion time courses reported here were obtained in the presence of 6-wt % PEG, which was sufficient to promote fusion of the charged vesicles but still left fusion of uncharged vesicles experimentally accessible. Fig. 1 shows time courses of LM, CM, and content L at 23°C of vesicles with increasing mole fractions of DOPS. DOPS content modulated both LM and CM, suggesting that DOPS did more than just impede the close approach of vesicle membranes. The parameters obtained from fitting the kinetic data to the single intermediate sequential model are presented in Table S1. The rates of intermediate formation (k_1) and pore formation (k_3) decreased continuously with increasing DOPS concentration in the membrane (Fig. 2, *inverted closed triangles*). The extents of LM and CM (%LM ~50%; %CM ~18–21%) changed insignificantly for DOPS contents up to 6 mol %, although there was a sharp drop in both at 8 mol % PS (Fig. 2, *C* and *D*). The probability that productive contacts led to transient pores in the intermediate (α_1) increased up to 6 mol % DOPS, except at 8 mol %, where both α_1 and β_1 dropped significantly (Fig. 2, *F* and *G*).

Comparison of DOPS and DOPG effects on PEG-mediated SUV fusion

Because our working hypothesis was that PS inhibits fusion because of its charge (10), we performed experiments with another acidic lipid, DOPG. Fig. 1 also includes representative time courses of LM, CM, and content L of vesicles with an increasing fraction of DOPG content. Analysis of these kinetic data led to the parameters presented in Table S2, with these plotted in Fig. 2 (*open triangles*) along with results for DOPS. The influence of DOPG on initial intermediate formation and LM were very similar to the effects of DOPS (Fig. 2, *A*, *C*, and *E*), except that DOPS inhibited the rate of I formation somewhat more effectively than did DOPG. To remove the complication that DOPG produced a somewhat more negative surface potential than DOPS in SUVs (Fig. S1), we also plotted k_1 in terms of surface potentials in the inset to Fig. 2 *A* and saw that it decreased linearly with surface potential for DOPG vesicles but more rapidly for DOPS vesicles. This suggests that the influence of DOPG on k_1 is related to surface potential, in agreement with our initial hypothesis (10), but that some other, headgroup-specific, effect contributes slightly for DOPS. The rate of pore formation (k_3) varied similarly (roughly quadratically) with DOPG or DOPS contents up to 6 mol % DOPS (Fig. 2 *B*), but did not vary similarly with the surface potentials of these two types of vesicles in that DOPS was more inhibitory at a given surface potential (Fig. 2 *B*, *inset*).

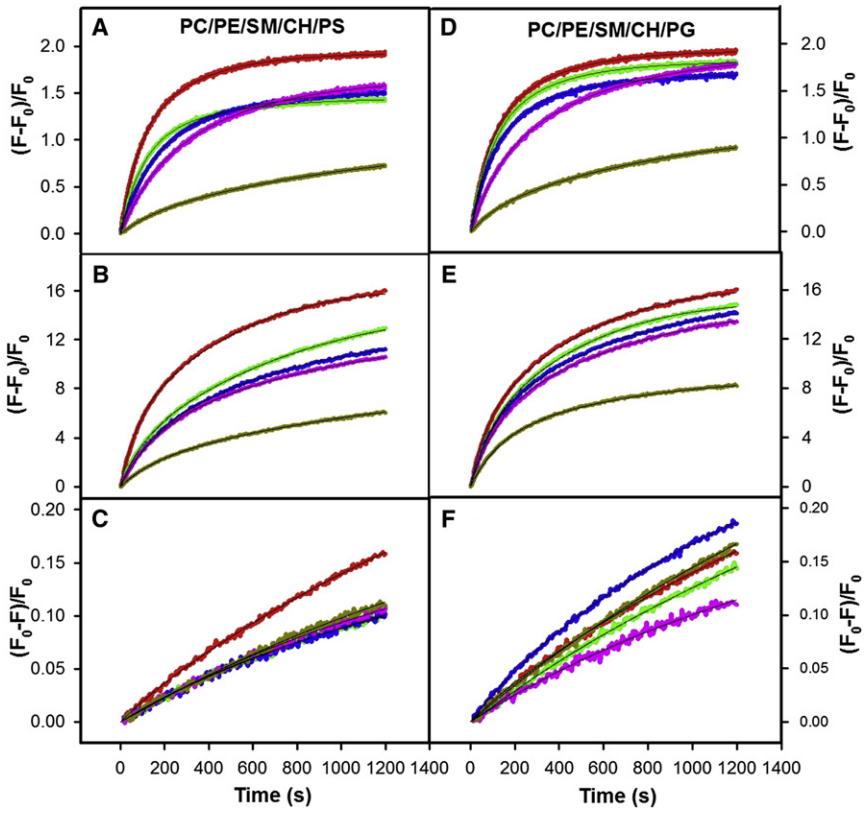

FIGURE 1 Effects of negatively charged lipids on fusion. Representative time courses (at 23°C) of 6 wt % PEG-induced (*A* and *D*) LM, (*B* and *E*) CM, and (*C* and *F*) L in SUVs (0.2 mM lipid) composed of DOPC/DOPE/SM/CH/DOPS (40-X:25:15:20:X) (*A*,*B*,*C*) or of DOPC/DOPE/SM/CH/DOPG (40-X:25:15:20:X) (*D*,*E*,*F*) in 10 mM TES, 100 mM NaCl, 1 mM ethylenediaminetetraacetic acid sodium, 1 mM $CaCl_2$ at pH 7.4. The smooth curves drawn through the data derive from the single-intermediate sequential model. The fitting parameters are shown in Table S1 and S2. Color code: red, 0 mol % PS/PG; green, 2 mol % PS/PG; blue, 4 mol % PS/PG; pink, 6 mol % PS/PG; drab green, 8 mol % PS/PG.

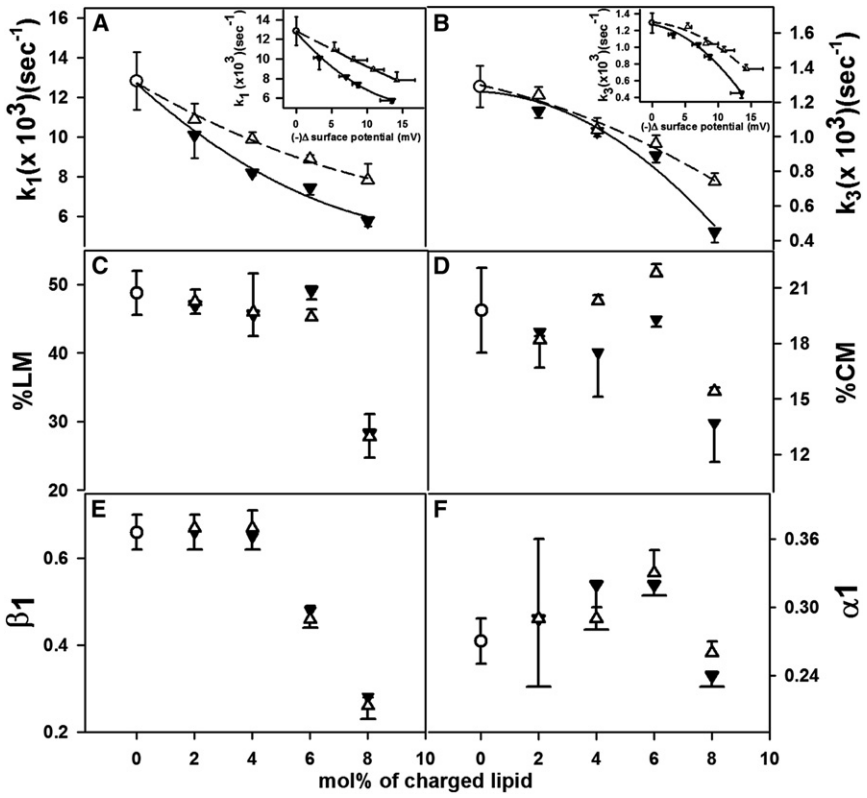

FIGURE 2 Effect of acidic lipids on the kinetics of the individual steps of fusion (frames *A* and *B*), on the extents of LM (frame *C*), and CM (frame *D*), and probabilities of LM (frame *E*) and CM (frame *F*) in the intermediate state. (*A*) Variation of k_1 with mol % of DOPS (▼) or DOPG (△) at 23°C. (*B*) Similar variation of k_3 with mol % of charged lipid. Inset to frames *A* and *B* show k_1 and k_3 as a function of membrane surface potential. All curves are quadratics drawn to guide the eye. (*C* and *D*) dependence of the extents of LM and CM on charged lipid content. (*E* and *F*) dependence of the probabilities of LM (β_1) and CM (α_1) in the fusion intermediate state with charged lipid content. Fusion was triggered by 6.0 wt % PEG. Total lipid concentration was 0.2 mM, the lipid composition was (DOPC/DOPE/SM/CH/DOPS (DOPG) at (40-X):25:15:20:X molar ratios) and the buffer contained 100 mM NaCl, 10 mM TES, 1 mM EDTA, and 1 mM calcium chloride. Experiments were carried out on different days with different sample preparations, and at least two time courses were obtained for each sample preparation, with a repeat performed when these did not appear consistent. Time courses were analyzed as described in the Methods, with final reported parameter values and their uncertainties (standard deviations) obtained by averaging results from these different analyses. Parameters from individual analyses generally fell within these error bounds, as expected for a normal distribution.

DOPS appeared as well to have a somewhat more inhibitory effect on the extent (%CM) of pore formation (Fig. 2 *D*).

Membrane physical properties

To ask whether DOPS might somehow influence outer leaflet or interfacial order, we examined the properties of a series of membrane probes that depend on interface and outer leaflet structure (22,23). The fluorescence anisotropy of DPH, the fraction of C_6NBD-PC in the membrane outer leaflet, the ratio of fluorescence lifetime of TMA-DPH incorporated into SUVs in D_2O versus H_2O buffers (τ_{D2O}/τ_{H2O}) were all found to be insensitive to the DOPS contents in a membrane from $X_{PS} = 0$ to 0.1 (data not shown). The decrease in TMA-DPH anisotropy at 8 and 10 mol % DOPS was however significant (Fig. S2), suggesting a unique ability of DOPS to disorder the interface in the physiological concentration range.

PEG-mediated vesicle aggregation

PEG is a hydrophilic polymer that promotes SUV aggregation by producing a layer of higher activity water at a vesicle surface that can be reduced by close contact between membranes. Increasing PEG concentration increases this osmotic effect and drives the membranes into even closer contact (24). To apply our model for fusion, the aggregation of vesicles should occur on a shorter timescale than intermediate formation and fusion. We monitored PEG-mediated vesicle aggregation kinetics by monitoring turbidity at 400 nm using a spectrophotometer. Rapid mixing of PEG with vesicles in a cuvette, using the same procedures we used to follow LM and CM experiments, revealed a very rapid rise in turbidity (Fig. 3 *A*) that could be described adequately only with three exponentials, yielding three rate constants: k_{fast}, k_{int}, and k_{slow}. Table S3 gives these constants as a function of DOPS vesicle content. There are two key observations derived from these data. First, the fast rate constant is roughly 20 times larger than k_1 values collected in Table S1, meaning that aggregation is much faster than the first step. This fast rate decreased as the DOPS content increased, as expected if electrostatics play a role in inhibiting vesicle aggregation, but $k_{fast} \gg k_1$ at all DOPS contents. We conclude that DOPS does not slow aggregation sufficiently that it becomes rate limiting in our measurement. Second, we note that k_{int} and k_{slow} approximate k_1 and k_3 for the fusion process, meaning that turbidity changes are likely due to membrane structural changes associated with intermediate and final pore formation during fusion, consistent with our original report that 90° light scattering is one of five observables that can be described by our fusion model without introducing additional rate constants (21). This interpretation is also consistent with our observation of a slow (normalized rates roughly equal to k_3) increase in mean particle diameter as fusion proceeds beyond the rapid formation of initial intermediate (Fig. 3 *B*). The data in

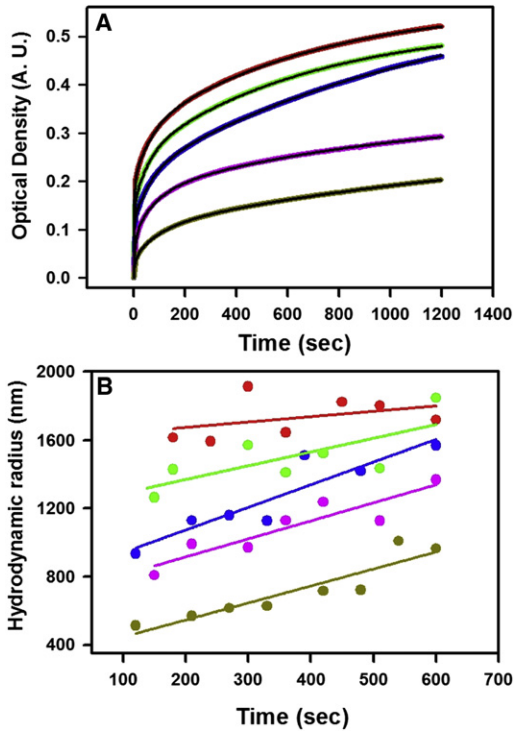

FIGURE 3 PEG-induced aggregation of vesicles at different mol % of PS. (*A*) Time dependence of sample turbidity at 400 nm for SUVs (see the Supporting Material) treated with 6% PEG at time 0. Samples and PEG stock were incubated 23°C before mixing (see Lipid Mixing Assay in the Supporting Material for details). The data were reasonably well described by the sum of three exponentials (*black lines*). (*B*) Average (assuming a single Gaussian distribution) hydrodynamic radii of vesicles treated with PEG as a function of time after PEG addition. Color code: red, 0 mol % DOPS; green, 2 mol % DOPS; blue, 4 mol % DOPS; pink, 6 mol % DOPS; drab green, 8 mol % DOPS.

frame *B* of Fig. 3 show that the size of the final fusion product decreased with increasing DOPS content, however, even at 8 mol % DOPS, aggregates were on the order of 1000 nm.

Increased PEG concentration overcomes the effect of charge

If the major effect of DOPS reported thus far at 6 wt %-PEG (Fig. 2) were to inhibit aggregation and close approach of membranes due to electrostatic repulsion, use of a higher concentration of PEG should then exert a larger osmotic pressure that might restore fusion to the extent seen in the absence of charged lipid. Fig. 4 shows that increasing PEG concentration increased the extents of LM and CM, k_1, k_3, and β_1. Indeed, increasing the aggregating concentration of PEG to roughly 7.5 wt % led to values of k_1, β_1, %LM, and %CM comparable to parameters obtained with vesicles lacking DOPS but aggregated by 6 wt % of PEG (Fig. 4). This is consistent with our hypothesis that a significant part of the inhibitory effect of DOPS on fusion is associated with electrostatic repulsion that can be overcome by an increased osmotic force.

Calcium plus acidic lipid promote PEG-mediated fusion of vesicles

Fig. 5 summarizes the effects of free calcium concentration on the kinetics of 6 wt % PEG-mediated fusion of SUVs containing 0% acidic lipid (▲), 8 mol % DOPS (●), or 8 mol % DOPG (○). The effects of Ca^{2+} on fusion of 0 mol % acidic lipid vesicles (▲) were minor as compared to effects on fusion of acidic-lipid-containing membranes. Calcium increased the rate of initial intermediate formation (k_1) at or above 0.2 mM in the presence of DOPS-containing membranes but had little effect on k_1 up to 0.4–0.5 mM for vesicles containing DOPG (Fig. 5 *A*). For neither lipid was Ca^{2+} able to recover k_1 values comparable to those observed in the absence of acidic lipid (Fig. 5 *A*). The extent of lipid mixing (%LM) between DOPS-containing vesicles increased most dramatically with Ca^{2+} concentration but plateaued by 0.4 mM, although it increased up to and beyond 0.9 mM for DOPG-containing vesicles, where %LM slightly exceeded that obtained with neutral lipid vesicles (Fig. 5 *C*). The fraction of total LM that occurs in the first intermediate state (β_1) increased for both DOPG-and DOPS-containing vesicles starting around 0.2 mM Ca^{2+}, with the increases in these quantities paralleling each other (Fig. 5 *E*). The ability of Ca^{2+} to increase the rate of pore formation (k_3) was roughly equal for vesicles containing either DOPS or DOPG, and this increase occurred over a broad range of Ca^{2+} concentrations (0.2 to 0.9 mM), leading to rates comparable to (DOPS) or perhaps greater than (DOPG) those observed in the absence of acidic lipid by 0.9 mM Ca^{2+} (Figs. 5 *B*). DOPS and to a lesser extent DOPG inhibited the extent of CM (Fig. 2 *D*), but Ca^{2+} relieved this inhibition dramatically in the range of 0.2 to 0.4 mM, especially for DOPS (Fig. 5 *D*). A most remarkable result is that the extent of content mixing (%CM) for DOPS-containing vesicles at high Ca^{2+} concentration was significantly larger than observed at that Ca^{2+} concentration in the absence of any acidic lipid, a result that was less evident for DOPG (Fig. 5 *D*).

We hypothesized that the role of Ca^{2+} was simply to allow closer apposition of vesicles. To test this, we used 7.5 wt % PEG to trigger fusion of 8 mol % DOPS vesicles at increasing Ca^{2+} concentrations (Fig. S5), expecting to find that this higher concentration of PEG would reduce the concentration of Ca^{2+} needed to overcome the inhibitory effect of DOPS or DOPG. Both k_1 and k_3 were higher in the presence of 7.5 wt % PEG as expected, however, surprisingly, the threshold Ca^{2+} concentration required for rate enhancement increased to ~0.7 mM from ~0.2 mM observed at 6 mol % PEG (Fig. 4, Fig. S5).

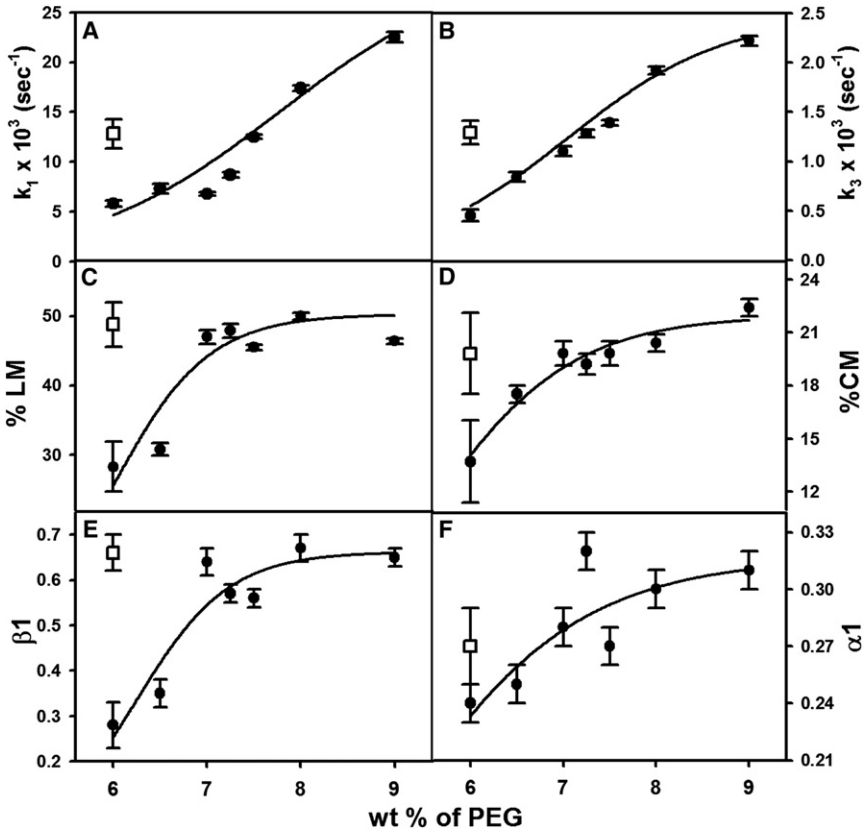

FIGURE 4 Effect of PEG concentration on the fusion kinetics of membranes containing 8 mol % DOPS. Frames show dependences of (*A*) k_1, (*B*) k_3, (*C*) % LM, (*D*) %CM, (*E*) β_1, and (*F*) α_1 on the concentration of PEG used to trigger fusion of vesicles (DOPC/DOPE/SM/CH/DOPS at 32:25:15:20:8 molar ratios) (*solid circles*). Open squares show values obtained with vesicles having 0 mol % (DOPS DOPC/DOPE/SM/CH at 40:25:15:20 molar ratios) at 6 wt % PEG. Buffer and lipid concentration are as in Fig. 2. Experiments were performed at least three times with analysis carried out on the combined time courses. Apparent outliers were always repeated. The errors presented in the figure are the parameter uncertainties from this combined analysis, although parameters from analysis of individual time courses normally fell within this range of uncertainty. The curves were obtained by fitting the data to sigmoidal or hyperbolic functions, whichever gave the best reduced χ^2 values. They are drawn to guide the eye and have no theoretical meaning.

DISCUSSION

Effects of acidic lipids

The results presented here show that, beyond a clear electrostatic influence, there appears to be an element of headgroup specificity in the effects of DOPS and DOPG on fusion. We note that acyl chain identity could affect fusion as well, but this is beyond the scope of the current study, in which we focused on the very simple species DOPC, DOPE, DOPG, and DOPS. A second significant conclusion is that acidic lipids influence initial intermediate and pore formation in different ways, thus, probably by different mechanisms. Acidic lipids reduced k_1 largely according to surface potential (modified to some extent by specific effects for DOPS), whereas k_3 decreased roughly with the square of acidic lipid content. The different effects of acidic lipid concentration on the probabilities of LM (β_1, Fig. 2 *E*) and CM (α_1, Fig. 2 *F*) in the intermediate state also support our contention that acidic lipids influence the processes of initial intermediate and pore formation differently. As for %LM, β_1 was unaffected by increasing mole fraction acidic lipid at low acidic lipid content, whereas α_1 increased up to 6 mol % acidic lipid. The dramatic drop in %LM and β_1 at 8 mol % acidic lipid likely caused the corresponding drop in %CM, because a pore cannot form without productive intervesicle contact. We note with interest that the cell membrane content of PS in many mammalian membranes is generally 8–10 mol %, exactly the concentration range in which acidic lipids significantly inhibited both productive intermediate and pore formation.

Effects of calcium in the presence of DOPS

We have come to three conclusions regarding the ability of Ca^{2+} to relieve acidic-lipid inhibition of PEG-mediated fusion. First, fairly low concentrations (0.2 to 0.4 mM) of Ca^{2+} overcame DOPS's inhibition of the extents of LM, CM, and the probability of LM in the intermediate (β_1) in the presence of 6 wt % PEG (Fig. 5, *C*, *D*, and *E*). These concentrations are well below the concentrations (1–5 mM) thought to be required to trigger fusion of PS-containing membranes (16–18), and are on the order of the free Ca^{2+} concentration reported to produce half maximal release of synaptic vesicles (~200 μM) (25). Although PEG (6 wt % for, membranes containing 8 mol % DOPS) is required to bring membranes into the 5 Å interleaflet separation needed to trigger fusion (9), it is reasonable to presume that PEG-mediated vesicle aggregation lowers Ca^{2+} concentrations needed to overcome the inhibitory effects of 8 mol % DOPS in our vesicle system. Fusion in vivo requires proteins that bring highly curved membranes into close contact with less curved membranes, whereas our studies use PEG to bring pairs of highly curved vesicles into close contact. Although it is generally believed

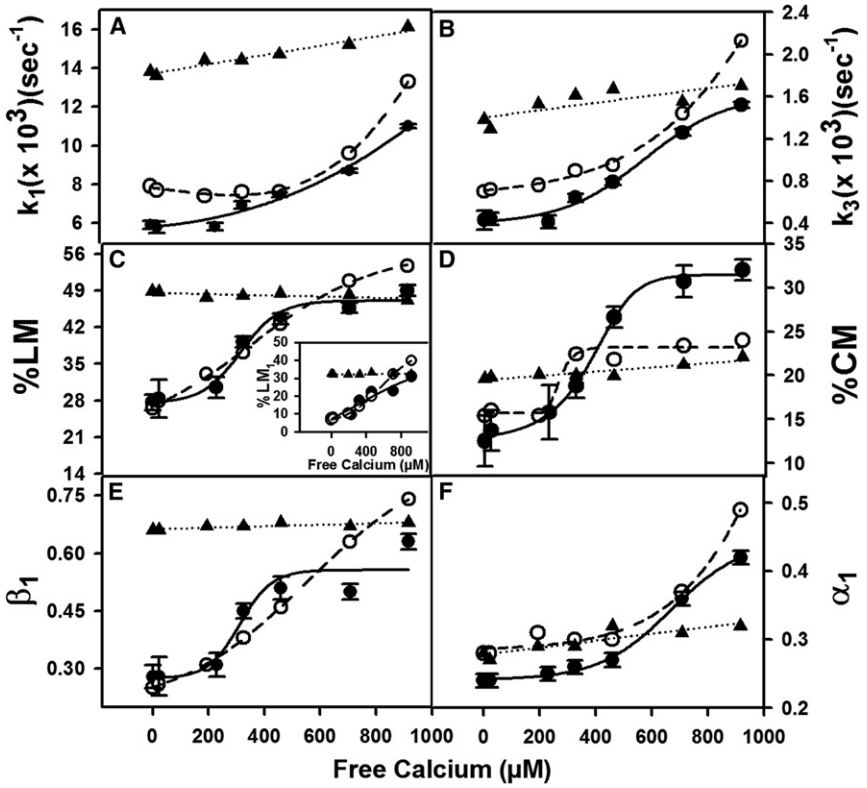

FIGURE 5 Effect of free calcium concentration on fusion of 8 mol % DOPS-(●), DOPG(○)-containing, or acidic-lipid-free (▲) vesicles triggered by 6 wt % PEG. SUVs at 0.2 mM total lipid (DOPC/DOPE/SM/CH/DOPS(DOPG); (32:25:15:20:8 molar ratios) in 100 mM NaCl, 10 mM TES, 1 mM EDTA were treated with 6.0 wt % PEG at 23°C and LM, CM, and L monitored with time to yield the Ca^{2+} dependence of (*A*) k_1, (*B*) k_3, (*C*) extent of expected lipid mixing (% LM), (*D*) extent of expected content mixing (% CM), (*E*) the probability of LM in the intermediate state (β_1), and (*F*) the probability of CM in the intermediate state (α_1). Free Ca^{2+} was determined as described in the Methods. The inset to frame C shows the quantity ($\beta_1 \cdot$% LM) = % LM_1, which represents the total amount of LM that occurs in the initial intermediate. Representative error bars are shown for DOPC/DOPE/SM/CH/DOPS sample. Experiments were performed at least three times with analysis carried out on the combined time courses. The errors presented in the figures are the parameter uncertainties from this combined analysis. Parameters from analysis of individual data sets also normally fell within this range of uncertainty. The curves were obtained as in Fig. 4 except that polynomial functions were also considered.

that the role of Ca^{2+} in synaptic vesicle release is to trigger changes in synaptotagmin (or other proteins) that then trigger fusion (26), the results presented here suggest that we should not rule out direct effects of Ca^{2+} on closely opposed membranes under appropriate conditions of close approach.

Second, whereas Ca^{2+} increased the rates of both initial intermediate and pore formation over a broader range of concentration, these rates never exceed those seen in the absence of acidic lipids. However, Ca^{2+} increased the extent of pore formation (%CM) between vesicles with 8 mol % DOPS well beyond that seen in the absence of PS and in a concentration range that is close to physiological (Fig. 5, *B* and *D*). The fact that %CM increased in a sharply sigmoidal fashion whereas α_1 increased over a broader range (Fig. 5, *D* and *F*) means that between 0.2 and 0.4 mM Ca^{2+}, the effect of Ca^{2+} was primarily to promote final pore formation, especially for DOPS-containing vesicles. The sigmoidal increase in β_1 for DOPS vesicles over the same concentration range (0.2 and 0.4 mM) is consistent with the expectation that a stable semifused intermediate state is needed before FP formation and that Ca^{2+} promotes formation of this in the presence of DOPS.

Third, Ca^{2+} does not function analogously to PEG in initial intermediate formation, i.e., by promoting a closer approach of bilayers containing PS. If it did, increasing the aggregating PEG concentration should have lowered the threshold Ca^{2+} concentration needed to promote the rate of intermediate formation, which it did not (Fig. S5 *A*). Indeed, this threshold increased significantly, suggesting that Ca^{2+} and PEG worked at opposite purposes in this instance. Because there are no reports of significant interactions between Ca^{2+} and PEG, our interpretation is that increased PEG concentration makes it more difficult for Ca^{2+} to reach the increasingly dehydrated and diminished interbilayer space where it can shield DOPS-DOPS or DOPG-DOPG repulsions and permit a closer approach of *cis* leaflets, as needed for formation of the transition state between the A and I state. Similarly, increasing the PEG concentration dramatically increases the Ca^{2+} threshold concentration at which the rate of final pore formation increased (Fig. S5 *B*). Although we have no clear interpretation of these opposing influences, this observation provides insight into possible molecular mechanisms by which Ca^{2+} influences the rate of pore formation. We conclude that the role of Ca^{2+} in fusion of PS-containing membranes goes well beyond reducing membrane-membrane electrostatic repulsion.

Mechanistic interpretations of effects of acidic lipids on fusion

Intermediate formation. We argue elsewhere on the basis of activation thermodynamics measurements that the transition state between the aggregated vesicle state (A) and the intermediate state involves lipid acyl chain movement into the dehydrated interbilayer space between contacting *cis* leaflets (1), as predicted by a recent molecular dynamics simulation (27). In the context of this mechanistic model, surface charge would limit close approach of the contacting

cis leaflets and should thus decrease the likelihood that two monolayers could get close enough to share lipid acyl chains (i.e., k_1 should decrease in proportion to surface potential, Fig. 2 *A*, *inset*). However, this occurred only for DOPG (Fig. 1 *A*, *inset*). The cause of the additional inhibitory effect of DOPS (Fig. 2 *A*, *inset*) is unknown, although we can suggest at least two possibilities. DOPS at pH 7.5 is triply charged (phosphate and carboxyl negative; amine positive) and under these conditions, the serine group extends away from the plane of the bilayer roughly parallel to the axis of the molecule to move it away from the phosphate (28). A molecular dynamics simulation also predicts such a conformation with extensive H-bonding associated with the amine of the serine headgroup, reducing the DPPS cross-sectional area in the bilayer and increasing acyl chain order (4). This extended conformation could not be stabilized by H-bonding for DOPG, suggesting that PS may provide an additional steric inhibition to close approach of fusing membranes. Water is also purported to be ordered in the interbilayer space at close interbilayer approach (29), and this ordering will certainly vary with the nature of acidic lipid headgroups present in the bilayers, although no specific data is available.

Productive intermediate stability. In contrast to k_1 and β_1, %LM decreased very little with acidic lipid content up to 6 mol %. Together these quantities define the probability of productive contacts between vesicles in the intermediate. This probability is a measure of thermodynamic stability of intermediate rather than the rate of reaching it. The intermediate state is generally viewed as having a structure in which contacting (*cis*) leaflets have merged but noncontacting (*trans*) leaflets have not, such that the merged *cis* leaflets experience significant negative curvature stress at the point of closest *cis* leaflet contact (stalk-like in Fig. S6). Because of electrostatic interactions, charged lipids partition into regions of positive curvature stress (30) and should avoid the negatively curved edge of the intermediate state. At low acidic lipid concentrations, this is easy to accomplish, but at increasing acidic lipid concentrations, the entropic cost of avoiding this edge region should overcome the enthalpic cost of occupying the region, explaining why the stability of intermediate could remain roughly unaffected by DOPS content up to 6 mol %, however, at 8 mol % acidic lipid, %LM dropped dramatically (Fig. 2 *C*).

Pore formation. The correlated lipid movement hypothesis for pore formation posits correlated movement of lipids into the hydrophobic defect region at the edge of the diaphragm intermediate structure (1). Lipid movement from unfused *trans* leaflets is assumed to correlate with movement of lipid from the joined *cis* leaflets is proposed to lower both interstice energy and reduce curvature stress at the same time, although at a large entropic cost (1). The transition state between the intermediate and final pore state is seen as involving a very large ensemble of structures called expanded *trans*-membrane contacts comprising a bilayer diaphragm separating two unfused compartments (ETMC in Fig. S6) (31). Expansion of this diaphragm is favored by decreased curvature stress but opposed by increasing unfavorable interstice energy (31). These correlated lipid movements/fluctuations are expected to be unfavorable due to movement of two or more acidic lipids with polar head and associated water molecules into a hydrophobic environment, but are possible because of the very large number of possible microstructures that can occur at the edge of the ETMC diaphragm. The probability of such correlated fluctuations should decrease in proportion to some power of acidic lipid content because of the electrostatic repulsion expected for two similarly charged headgroups. This offers a reasonable explanation for why k_3 decreases roughly quadratically with acidic lipid content except at 8 mol % DOPS, which is more inhibitory than DOPG (Fig. 2 *B*). Reported H-bond-mediated intermolecular interactions between PS headgroups (4,28,32) would presumably make correlated movement of only two PS molecules more difficult at higher DOPS content, potentially limiting the number of microstructures contributing to the transition state ensemble, thus further decreasing k_3. Increased PEG concentration creates a compressive force (33) that can potentially be accommodated by movement of lipid into interstices (31) and reducing interstice energy, this will tend to expand the ETMC diaphragm. This expansion increases the edge circumference at which fluctuations can occur and should thus provide a favorable entropic contribution to I $\rightarrow$ FP transition state formation, leading to an increase in k_3. Thus, according to our model of this transition, increasing PEG concentration overcomes the inhibitory influence of DOPS.

Mechanistic interpretations of effects of calcium on fusion of DOPS-containing vesicles

Intermediate formation. Ca^{2+} increased k_1 of PEG-mediated fusion of DOPS- and DOPG-containing vesicles (Fig. 5, *A* and *B*), but not to the values in the absence of acidic lipid (Fig. 5 *A*). Because DOPG inhibition of step 1 appeared to be primarily electrostatic in nature, we presume that Ca^{2+} might to some extent penetrate the interbilayer space and reduce this effect. We have shown that the effects of DOPS are not simply electrostatic in nature and there is no reason to expect that Ca^{2+} and DOPS would work in concert according to this simple picture. So, how might Ca^{2+} modulate the mechanism of intermediate formation differently for DOPS-containing versus DOPG-containing membranes? Ca^{2+} induces $(PS)_2Ca^{2+}$ complexes between bilayers (34) and within bilayers (35), leading to microclustering. The intrabilayer complex limits the conformational freedom of PS to mainly two slowly interchanging conformations that occur in each complex. The interbilayer complex promotes a dehydrated chocolate phase long known to be the end product of mixing Ca^{2+} with pure PS vesicles. In either case, PS headgroups become condensed in the complex, whereas acyl chains remain quite fluid

(34,35). Although no data exist on headgroup condensation of DOPG due to association with Ca^{2+}, one presumes that Ca^{2+} might produce at least some headgroup condensation, although probably not to the extent documented for PS. In the acyl-chain protrusion model for the A → I transition state (1), close approach of bilayers leads to many energetically unfavorable and entropically favorable microstructures in which single acyl chains migrate from monolayer interiors into the partially dehydrated interbilayer space and into the adjacent monolayer. Headgroup condensation should increase the exposure of acyl chains to water in membranes and promote this phenomenon. This is expected to decrease the free energy required for a fluctuation of an acyl chain into the interbilayer space. By this reasoning, one might expect that Ca^{2+} would promote intermediate formation between DOPS-containing membranes at rates as large as and perhaps larger than those seen for DOPG, which is not the case. However, Chakraborty et al. (1) proposed that a wide range of similar microstructures contributes to the transition state ensemble for step 1, resulting in large activation entropy that partially overcomes unfavorable enthalpic effects and makes intermediate formation possible on a reasonable timescale. Because PS in the PS_2-Ca^{2+} complex has reduced conformational mobility, this may explain why Ca^{2+} cannot promote intermediate formation at a rate even greater than for bilayers containing DOPG. We conclude that the acyl chain protrusion model for the initial fusion transition state offers a reasonable mechanistic interpretation of our results for the effects of Ca^{2+} on fusion with both acidic lipids.

Productive intermediate stability. Although acidic lipids had little or no inhibitory influence on the formation of productive intermediates at low acidic lipid contents, Ca^{2+} increased the extent of lipid mixing (%LM; Fig. 5 *C*) and made LM more likely early in the fusion process (increased β_1; Fig. 5 *E*), meaning that Ca^{2+} favored formation of productive intermediates in the presence of acidic lipids. Of particular interest is the fact that, although this occurred over a broad range of Ca^{2+} concentration for DOPG, it occurred with DOPS over a physiologically relevant concentration range. This can be understood in terms of the same concepts of extreme negative curvature stress at the edges of the stalk intermediate. The ability of Ca^{2+} to form intralamellar PS_2Ca^{2+} complexes with reduced headgroup cross section should significantly stabilize the intermediate. The fact that DOPG does not form stoichiometric complexes likely accounts for why the stability of the fusion intermediate for DOPG-containing vesicles increases less dramatically with Ca^{2+} concentration than is the case for DOPS vesicles.

Pore formation. As discussed, the correlated lipid movement hypothesis explains the inhibitory effects of acidic lipids on pore formation in terms of the increased energy needed for correlated movements of charged headgroups into the hydrophobic regions at the stressed edge of the purported intermediate structure (1). Counter ions that reduce this energy will reduce this inhibition. The ability of Ca^{2+} to associate with and lower the zeta potential of negatively charged or even neutral lipid membranes (36) is thus consistent with its ability to increase the rate of pore formation in such membranes (Fig. 5 *B*). The slight sigmoidal shape of the curve for Ca^{2+} effects on k_3 for DOPS-containing vesicles (Fig. 5 *B*) could again reflect the ability of PS to form an intraleaflet PS_2Ca^{2+} stoichiometric complex with DOPS (35) but not for DOPG, for which stoichiometric complexes have not been reported.

Fusion pore stability. An important aspect of our results is the extent to which Ca^{2+} promotes pore formation between vesicles containing 8 mol % DOPS. Although pore formation between DOPG-containing vesicles was also affected, the %CM for DOPS-containing vesicles increased in a sharply sigmoidal fashion to a value nearly twice that seen for neutral lipid vesicles in the absence of Ca^{2+} (Fig. 5 *D*). Certainly, the sigmoidal increase in %LM with Ca^{2+} concentration for DOPS-containing vesicles is in part responsible for this result, because a productive intermediate is a requirement for fusion pore formation. Although the probability of formation of transient pores in the intermediate state (α_1) also increased, most of the increase was associated with formation of stable pores in FP, indicating that this result is not simply due to stability of productive intermediates. We speculate that an initial pore still has an extremely negatively curved *cis* leaflet, which is stabilized by DOPS headgroup condensation. In addition, initial pores must also have acidic lipid headgroups along with their associated water occupying a significantly hydrophobic environment (37). Intraleaflet or interleaflet PS_2Ca^{2+} complex microstructures, as have been proposed (34,35), could stabilize such structures so they can expand into larger, more stable pores.

Relationship to biomembrane fusion. The most remarkable aspect of our results is that most of the increase in the extent of CM occurs at a fairly low, Ca^{2+} concentration (0.2–0.4 mM), close to those known to be physiologically significant. PS is the most abundant acidic lipid in mammalian neuronal cell membranes (and in many other mammalian membranes), whereas Ca^{2+} is widely recognized as the trigger of neuronal release. Although binding of Ca^{2+} with regulatory fusion proteins is still very likely key to the mechanism of triggering fusion in vivo, our results make it difficult to ignore the possibility that the unique physical properties of this ion-lipid pair may play more significant roles in fusion in vivo than is currently envisioned.

SUPPORTING MATERIAL

Additional research and supporting references are available at http://www.biophysj.org/biophysj/supplemental/S0006-3495(12)01071-5.

This work was supported by U.S. Public Health Service grant GM32707 to B.R.L.

REFERENCES

1. Chakraborty, H., P. K. Tarafdar, …, B. R. Lentz. 2012. Activation thermodynamics of poly(ethylene glycol)-mediated model membrane fusion support mechanistic models of stalk and pore formation. *Biophys. J.* 102:2751–2760.
2. Yeung, T., G. E. Gilbert, …, S. Grinstein. 2008. Membrane phosphatidylserine regulates surface charge and protein localization. *Science.* 319:210–213.
3. Jones, M. E., and B. R. Lentz. 1986. Phospholipid lateral organization in synthetic membranes as monitored by pyrene-labeled phospholipids: effects of temperature and prothrombin fragment 1 binding. *Biochemistry.* 25:567–574.
4. Pandit, S. A., and M. L. Berkowitz. 2002. Molecular dynamics simulation of dipalmitoylphosphatidylserine bilayer with Na+ counterions. *Biophys. J.* 82:1818–1827.
5. Kozlov, M. M., S. L. Leikin, …, Y. A. Chizmadzhev. 1989. Stalk mechanism of vesicle fusion. Intermixing of aqueous contents. *Eur. Biophys. J.* 17:121–129.
6. Siegel, D. P. 1999. The modified stalk mechanism of lamellar/inverted phase transitions and its implications for membrane fusion. *Biophys. J.* 76:291–313.
7. Lentz, B. R., V. Malinin, …, K. Evans. 2000. Protein machines and lipid assemblies: current views of cell membrane fusion. *Curr. Opin. Struct. Biol.* 10:607–615.
8. Chernomordik, L., M. M. Kozlov, and J. Zimmerberg. 1995. Lipids in biological membrane fusion. *J. Membr. Biol.* 146:1–14.
9. Burgess, S. W., T. J. McIntosh, and B. R. Lentz. 1992. Modulation of poly(ethylene glycol)-induced fusion by membrane hydration: importance of interbilayer separation. *Biochemistry.* 31:2653–2661.
10. Haque, M. E., T. J. McIntosh, and B. R. Lentz. 2001. Influence of lipid composition on physical properties and peg-mediated fusion of curved and uncurved model membrane vesicles: "nature's own" fusogenic lipid bilayer. *Biochemistry.* 40:4340–4348.
11. Deutsch, J. W., and R. B. Kelly. 1981. Lipids of synaptic vesicles: relevance to the mechanism of membrane fusion. *Biochemistry.* 20:378–385.
12. Bhalla, A., W. C. Tucker, and E. R. Chapman. 2005. Synaptotagmin isoforms couple distinct ranges of Ca2+, Ba2+, and Sr2+ concentration to SNARE-mediated membrane fusion. *Mol. Biol. Cell.* 16:4755–4764.
13. Martin, I., and J. M. Ruysschaert. 1997. Comparison of lipid vesicle fusion induced by the putative fusion peptide of fertilin (a protein active in sperm-egg fusion) and the NH2-terminal domain of the HIV2 gp41. *FEBS Lett.* 405:351–355.
14. Williams, D., J. Vicôgne, …, J. E. Pessin. 2009. Evidence that electrostatic interactions between vesicle-associated membrane protein 2 and acidic phospholipids may modulate the fusion of transport vesicles with the plasma membrane. *Mol. Biol. Cell.* 20:4910–4919.
15. Dennison, S. M., M. E. Bowen, …, B. R. Lentz. 2006. Neuronal SNAREs do not trigger fusion between synthetic membranes but do promote PEG-mediated membrane fusion. *Biophys. J.* 90:1661–1675.
16. Papahadjopoulos, D., G. Poste, …, W. J. Vail. 1974. Membrane fusion and molecular segregation in phospholipid vesicles. *Biochim. Biophys. Acta.* 352:10–28.
17. Portis, A., C. Newton, …, D. Papahadjopoulos. 1979. Studies on the mechanism of membrane fusion: evidence for an intermembrane Ca2+-phospholipid complex, synergism with Mg2+, and inhibition by spectrin. *Biochemistry.* 18:780–790.
18. Wilschut, J., and D. Papahadjopoulos. 1979. Ca2+-induced fusion of phospholipid vesicles monitored by mixing of aqueous contents. *Nature.* 281:690–692.
19. Feigenson, G. W. 1986. On the nature of calcium ion binding between phosphatidylserine lamellae. *Biochemistry.* 25:5819–5825.
20. Ginsberg, L. 1978. Does Ca2+ cause fusion or lysis of unilamellar lipid vesicles? *Nature.* 275:758–760.
21. Weinreb, G., and B. R. Lentz. 2007. Analysis of membrane fusion as a two-state sequential process: evaluation of the stalk model. *Biophys. J.* 92:4012–4029.
22. Haque, M. E., H. Chakraborty, …, B. R. Lentz. 2011. Hemagglutinin fusion peptide mutants in model membranes: structural properties, membrane physical properties, and PEG-mediated fusion. *Biophys. J.* 101:1095–1104.
23. Lee, J. K., and B. R. Lentz. 1997. Outer leaflet-packing defects promote poly(ethylene glycol)-mediated fusion of large unilamellar vesicles. *Biochemistry.* 36:421–431.
24. Lentz, B. R. 2007. PEG as a tool to gain insight into membrane fusion. *Eur. Biophys. J.* 36:315–326.
25. Heidelberger, R., C. Heinemann, …, G. Matthews. 1994. Calcium dependence of the rate of exocytosis in a synaptic terminal. *Nature.* 371:513–515.
26. Brose, N., A. G. Petrenko, …, R. Jahn. 1992. Synaptotagmin: a calcium sensor on the synaptic vesicle surface. *Science.* 256:1021–1025.
27. Kasson, P. M., E. Lindahl, and V. S. Pande. 2010. Atomic-resolution simulations predict a transition state for vesicle fusion defined by contact of a few lipid tails. *PLOS Comput. Biol.* 6:e1000829.
28. Sanson, A., M. A. Monck, and J. M. Neumann. 1995. 2D 1H-NMR conformational study of phosphatidylserine diluted in perdeuterated dodecylphosphocholine micelles. Evidence for a pH-induced conformational transition. *Biochemistry.* 34:5938–5944.
29. Kasson, P. M., E. Lindahl, and V. S. Pande. 2011. Water ordering at membrane interfaces controls fusion dynamics. *J. Am. Chem. Soc.* 133:3812–3815.
30. Lentz, B. R., D. R. Alford, and F. A. Dombrose. 1980. Determination of phosphatidylglycerol asymmetry in small, unilamellar vesicles by chemical modification. *Biochemistry.* 19:2555–2559.
31. Malinin, V. S., and B. R. Lentz. 2004. Energetics of vesicle fusion intermediates: comparison of calculations with observed effects of osmotic and curvature stresses. *Biophys. J.* 86:2951–2964.
32. Browning, J. L., and J. Seelig. 1980. Bilayers of phosphatidylserine: a deuterium and phosphorus nuclear magnetic resonance study. *Biochemistry.* 19:1262–1270.
33. Malinin, V. S., P. Frederik, and B. R. Lentz. 2002. Osmotic and curvature stress affect PEG-induced fusion of lipid vesicles but not mixing of their lipids. *Biophys. J.* 82:2090–2100.
34. Roux, M., and M. Bloom. 1991. Calcium binding by phosphatidylserine headgroups. Deuterium NMR study. *Biophys. J.* 60:38–44.
35. Boettcher, J. M., R. L. Davis-Harrison, …, C. M. Rienstra. 2011. Atomic view of calcium-induced clustering of phosphatidylserine in mixed lipid bilayers. *Biochemistry.* 50:2264–2273.
36. Mosharraf, M., K. M. Taylor, and D. Q. Craig. 1995. Effect of calcium ions on the surface charge and aggregation of phosphatidylcholine liposomes. *J. Drug Target.* 2:541–545.
37. Knecht, V., and S. J. Marrink. 2007. Molecular dynamics simulations of lipid vesicle fusion in atomic detail. *Biophys. J.* 92:4254–4261.